

Effect of Particle Size Distribution on Processing and Properties of Metal Injection Moulded 4140 and 4340

Andrew J Coleman, Keith Murray, Martin Kearns, Toby A. Tingskog*,
Bob Sanford** & Erainy Gonzalez**

Sandvik Osprey Ltd., Red Jacket Works, Milland Road, Neath, SA11 1NJ, UK

*Sandvik Osprey Ltd., USA

** TCK S.A., Zona Franca Industrial Las Americas, Santo Domingo, Dominican Republic

ABSTRACT

The popularity of low alloy steels within the MIM industry has grown over recent years such that today they are used in a wide range of general engineering applications and manufacture of gun parts. A variety of different raw materials mixes and processing routes has been developed by different MIM houses to meet the required product specifications. In this study, we compare the processing and properties of 4140 and 4340 steel parts made using gas atomized prealloy powders at 90%-16 μ m and 90%-22 μ m and a 3x concentration master alloy powder (90%-22 μ m) blended with carbonyl iron powder. The differences in densification behavior are evaluated for each alloy and the microstructure – property relationships for four different sintering temperatures are established with respect to tensile properties and hardness trends.

INTRODUCTION

Low alloy steels remain in widespread use in the MIM industry today continuing the initial success of carbonyl iron based MIM feedstocks in the early 1980s [1]. They offer high strength and toughness and are cost effective in many applications including general engineering, automotive components and gun parts. AISI 4140(FeCrMnMoC) and 4340(FeNiCrMnMoC) are two of the more popular grades used in the industry. MIM components produced using these alloys are used in the as-sintered or higher strength heat treated condition depending on service requirements. There are a number ways of producing these alloys using different powder routes; 1) Prealloyed (PA) powder of the desired composition, 2) Carbonyl Iron powder (CIP) + master alloy (MA, typically 3x concentration), and 3) CIP + FeCr + FeMo (+FeNi or carbonyl Ni) MAs.

MAs are often used in the MIM industry as they have been shown to offer a number of benefits for some alloy systems though little has been published on low alloy steel MA [2,3]. In particular the chemistry can be controlled within narrower chemistry ranges and composition can be refined to complement carbon and oxygen content in the CIP. The use of fine CIP powder blended with coarser MA particles has been shown to significantly improve green strength and reduce distortion in sintered parts [2]. Use of fine CIP powder with MA has been shown to facilitate activation of sintering at lower temperatures, improve finished densities and mechanical properties. From a commercial viewpoint, use of MA offers potential cost savings, particularly for low alloy steels, in terms of raw material costs as well as the potential processing and property benefits outlined above.

Published data showing wrought properties and reported as-sintered and heat treated MIM parts are shown in Table 1 for alloy 4140 and in Table 1 for 4340 [4-8]. These show that big differences in properties exist between the as-sintered and heat treated parts.

Table 1: Published values for Alloy 4140 [4-7].

4140	EPMA[4]			BASF[5]		MIMA Handbook		German & Bose[6]		Wrought Properties[7]	
	AS	HT	HT	AS	HT	Q&T typ	Q&T min	AS	HT	Ann'l 815C	Temper 205F
% density				>94		95		97	93	100	100
0.2%YS MPa, ksi	400 (58)	600 (87)	1200 (174)	400 (58)	1250 (181)	1240 (180)	1070 (155)	390 (57)	1240 (180)	417 (60)	1641 (238)
UTS MPa, ksi	700 (102)	750 (109)	1300 (189)	650 (94)	1450 (210)	1650 (240)	1380 (200)	580 (84)	1380 (200)	655 (95)	1772 (257)
%EI	3	3	2	3	2	5	3	15	2	25	8
Hardness HRC		25	50	18	45	46	46	18	40		

Table 2: Published values for Alloy 4340 [4,6-8].

4340	EPMA[4]			BASF[8]		German & Bose[6]		Wrought Properties[7]	
	AS	HT	HT	AS	HT	AS	HT	Ann'l 810C	Temper 205C
% density				>95		96	96	100	100
0.2%YS MPa, ksi		750 108	1400 203	500 73	1250 181	480 70	1400 203	472 69	1675 243
UTS MPa, ksi		900 131	1600 232	700 102	1450 210	620 90	1600 232	745 108	1875 272
%EI		3	2	7	2	6	2	22	10
Hardness HRC		25	48	20	45	20	48		

This paper explores sintering and properties of parts made from 4140 and 4340 PA powders using two particle size distributions (90%-22 μ m and 90%-16 μ m) and compares this data with parts made from a 3x MA blended with CIP powder. The effect of sintering temperature on microstructural and mechanical properties is reviewed.

EXPERIMENTAL PROCEDURE

Low alloy steel 4140 and 4340 powders were produced by Sandvik Osprey's proprietary inert gas atomization process using nitrogen gas. For the purposes of this paper, PA refers to powder that is produced to the final low alloy steel composition, whereas MA refers to atomized powder produced with high concentrations of alloying elements that must be subsequently diluted by blending with CIP to produce the same nominal low alloy steel composition. The chemistry of the powder batches is shown in Table 3.

Table 3: Chemical specification and measured analysis for 4140 & 4340 (as atomized powders)

Element	4140 Spec. (%)	PA (%)	MA (%)	MA+CIP	4340 Spec. (%)	PA (%)	MA (%)	MA+CIP
Fe	Bal.	Bal.	Bal.	Bal.	Bal.	Bal.	Bal.	Bal.
Ni		na	na	na	1.65-2.00	1.9	5.4	1.80
Cr	0.8-1.0	1.02	3.1	1.03	0.7-0.9	0.82	2.5	0.83
C	0.35-0.5	0.43	1.38	0.47	0.38-0.43	0.43	0.017	0.57
Si	0.15-0.35	0.26	0.92	0.31	0.15-0.35	0.15	0.73	0.24
Mn	0.75-1.0	0.84	2.7	0.89	0.6-0.8	0.76	1.8	0.59
Mo	0.15-0.25	0.25	0.63	0.21	0.2-0.3	0.24	0.77	0.26
P		0.01	0.016	0.005	0.03	na	0.007	0.002
S		0.008	0.007	0.002	0.03	na	0.005	0.002
O		0.125	na	0.2		na	na	0.19
N		na	na	0.003		na	na	0.5

From the as atomized PA powder two different size fractions were extracted via air classification, namely 90% -22 μ m and 90%-16 μ m. The same tap density values were measured for both PA powders of 4140 and 4340. Tap density values were 4.9g/cm³ and 4.85g/cm³ for 90%-22 μ m and 90%-16 μ m respectively. The MA powder was atomized and sized to a distribution of 90%-22 μ m. This MA powder was subsequently blended with CIP powder obtained from Sintez (CIP Grade BC powder) having chemistry: 0.016% C, 0.426% O, 0.008% N and 0.0006% S and particle size distribution, D₁₀ 3.0 μ m, D₅₀ 6.2 μ m and D₉₀ 14.0 μ m. The blend was produced in order to satisfy the respective ASTM 4140 and 4340 specifications. Table 4 shows the particle size distribution data for the PA and MA + CIP 4140 powder along with melt flow index (MFI) values. There is little difference between the D₁₀ values for the 90%-22 μ m and 90% 16 μ m powders but these differences become more apparent at the coarse end of the particle size distribution as expected. The MA+CIP powder is the finest of the powders used and actually meets a 90%-15 μ m specification. Similar particle size distributions and viscosity values were observed for the corresponding 4340 powder used in this study.

Table 4: Particle size data and melt flow index (MFI) values for 4140 alloy feedstock (61.8% v/v)

Particle size (μ m)	D10 μ m	D50 μ m	D90 μ m	MFI(g/min)
Prealloy 90%-22 μ m	4.4	10.5	21.5	402
Prealloy 90%-16 μ m	4.5	8.8	15.8	305
MA+CIP(90%-15 μ m)	2.9	6.9	14.5	106

Feedstock and Parts Manufacture

Six feedstock batches were compounded using PA and MA+CIP powders by TCK using their proprietary multicomponent wax/polymer binder system. The same metal loading of 61.8vol% was used for all feedstocks used in this study. Feedstocks were checked for viscosity using a melt viscometer. Viscosity values are shown for alloy 4140 in Table 4. For both alloys the viscosity of the PA powder increased with decreasing particle size. The MAs of both 4140 and 4340 exhibited significantly higher viscosity values than the PA powders. This is attributed to the large amount of fine CIP powder present in the MA mixes. The feedstocks were injection molded (Arburg) and sintered by TCK, to produce MIMA standard tensile and Charpy bar test specimens.

Sintering

Green parts were subject to an initial solvent debind followed by a thermal debind at 500°C (932°F) and sintered in a nitrogen atmosphere. Sintering was carried out in the range 1000°C to 1300°C (1832-2372°F) with a holding time at the sintering temperature of 2h. Sintered parts were allowed to slow cool under a

nitrogen atmosphere. As-sintered tensile samples were kept for triplicate testing and further samples were solutionized for 60min [850°C (1562°F) for 4140 and 830°C (1526°F) for 4340], oil quenched and tempered at 1h at 250°C followed by air cooling. The heat treatment parameters were chosen to achieve peak hardness following initial heat treatment trials over a range of tempering temperatures. Tensile testing was carried out on three specimens in each condition in accordance with ASTM E8-08. Vickers hardness testing was carried out using a 10kg weight. Sintered density measurements were carried out using a Micromeritics Accupyc II1340 Helium Pycnometer and also calculated from sample dimensions and weights. Polished cross-sections of Charpy bars were prepared for porosity measurements and microstructures were analysed in the polished and etched (3% Nital) conditions. In order to evaluate distortion during sintering, Charpy test bars were suspended across refractory supports, separated by 38mm in the sintering furnace as shown in Fig. 1a. After sintering, images of the deflection of the Charpy bars were captured.

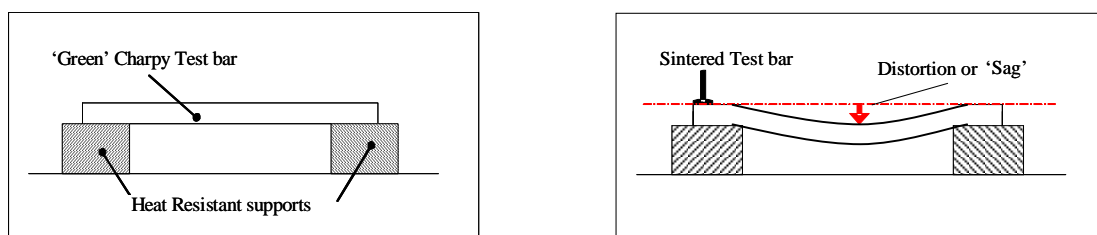


Figure 1: a), Distortion test configuration and b), example of distortion after sintering

RESULTS

As-sintered parts were analyzed for C content to confirm that the final C content fell within the target specification of 0.35-0.5%. Values of 0.39%, 0.39% and 0.38% C were observed for 90%-22 μ m, 90%-16 μ m and MA+CIP 4140 following sintering at 1100°C. From this it is evident that C content was well controlled for all powder variants at this temperature and remained within specification. Similar data were obtained for the other sintering temperatures used in this study.

Densification

Density values measured Pycnometrically and calculated from Charpy bar dimensions and weights are compared for different sintering temperatures in Figure 2. The two different measurement techniques suggest rather different trends in density which is not altogether unexpected. Calculated density is observed to increase with sintering temperature for each powder particle size. The MA+CIP powder samples have the highest density for all sintering temperatures, followed by 90%-16 μ m and 90%-22 μ m PA powders. Pycnometric density values are high for all samples sintered at 1000°C (1832°F) suggesting full densification but these are misleading and are actually indicative of interconnected porosity. What is apparent from subsequent data for increasing sintering temperatures is that interconnected porosity is removed from the MA+CIP powder at 1100°C for alloy 4140, whereas this does not occur until 1200°C (2192°F) for the 90%-16 μ m powder and 1300°C for 90%-22 μ m powder. This is evidence of the faster sintering rates exhibited by finer powders. In the case of 4340 interconnected porosity appears to have been removed for both the MA+CIP and 90%-16 μ m powders at 1100°C (2012°F) and from 90%-22 μ m powder at 1200°C (2192°F). The difference in absolute density values measured by the different techniques at 1300°C (2372°C), where one would expect convergence, is taken as evidence that the dimensional measurements systematically overestimate the volume of samples.

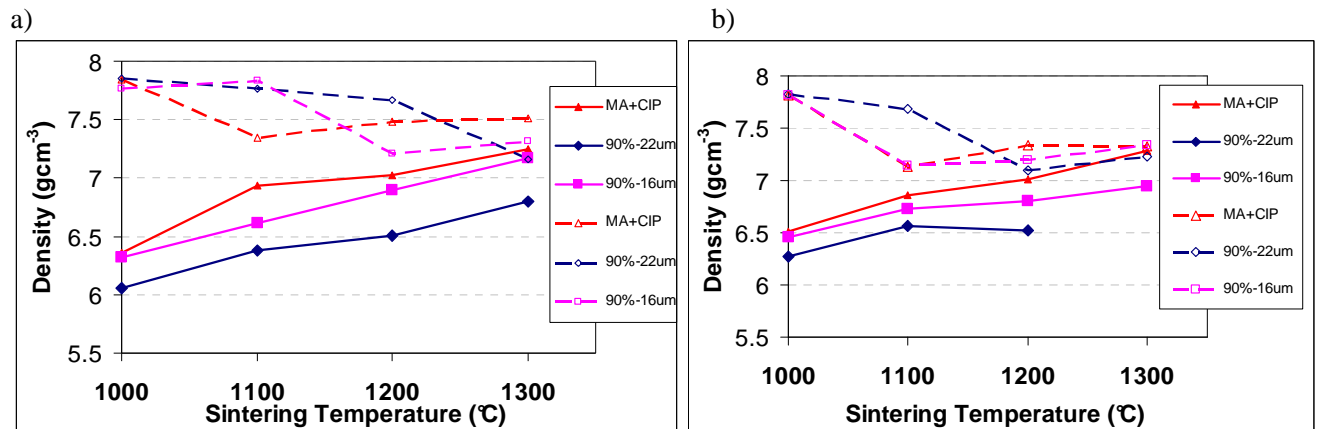


Figure 2: Density data for a) alloy 4140 and b) 4340 vs. sintering temperature. Hollow symbols are pycnometric data; Solid symbols by calculation from weight & dimensions

After furnacing, cross-sections of Charpy bars were prepared for metallographic analysis of both the as-polished and etched surfaces. Porosity measurements are summarized in Figure 2 for alloys 4140 and 4340. This figure shows higher densification rates for the MA+CIP variant compared with PA with increasing sintering temperature. The highest final density value (4% porosity) for alloy 4140 is observed for the MA+CIP powder and confirms results in Fig.2. In the case of 4340 the MA+CIP variant also exhibited higher densification rates but maximum density (<7% porosity) was achieved there at 1200°C. The pycnometric and calculated density values for 4340 showed an increase in density between 1200°C and 1300°C to a maximum value of $\sim 7.28\text{gcm}^{-3}$ (>92% of theoretical density) at 1300°C.

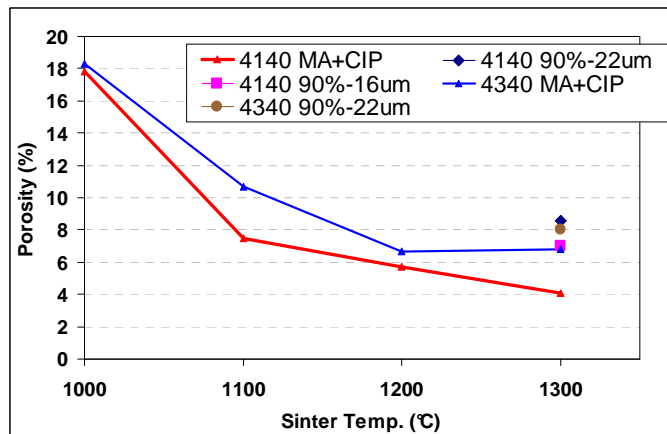


Figure 3: Porosity measurements for alloy 4140 from metallographic analysis.

Etched microstructures were analysed for both alloys. Figure 4 shows the change in as-sintered microstructure for parts produced using 4140 MA+CIP as a function of sintering temperature: a), 1000°C b), 1100°C c), 1200°C and d), 1300°C. At the lower sintering temperatures (1000 - 1100°C) a relatively even distribution of pearlite and austenite is observed with the primary difference being a coarsening of the grain size at 1100°C. There appears to be slightly more pearlite (not measured) at 1000°C and the structure of the pearlite varies at both 1000°C and 1100°C depending on the time available for transformation. A more significant change is observed after sintering at 1200°C where a non-uniform distribution of bainite and pearlite is observed. Bainite is the primary phase with small

islands of pearlite and no residual austenite. At 1300°C, the microstructure is almost wholly bainitic with some pearlite only at the surface.

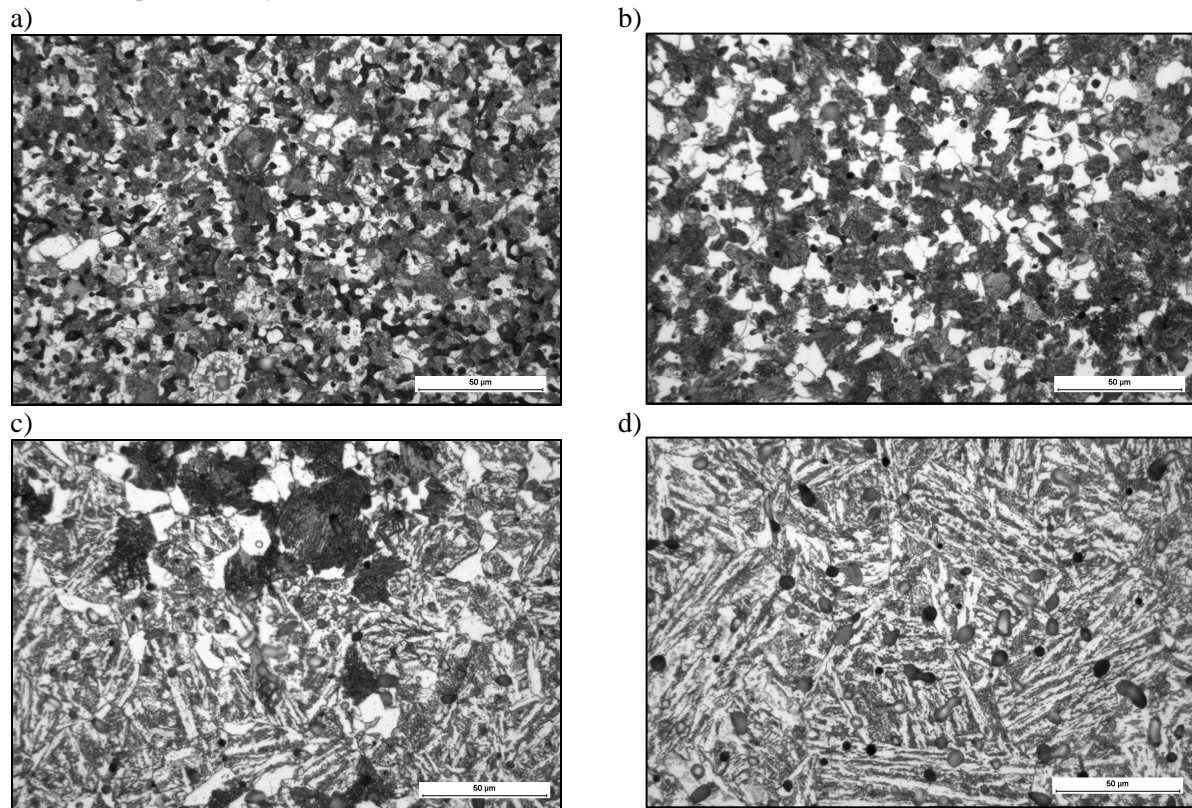


Figure 4: shows the effects of changing sintering temperature on as-sintered microstructure of MA+CIP 4140 a), 1000°C b), 1100°C c), 1200°C and d), 1300°C

The Time-Temperature-Transformation (TTT) diagram for alloy 4140 (shown in Figure 5a) helps explain the different appearance of the microstructures shown in Figure 4. Cooling from 1000°C and 1100°C allows insufficient time for transformation to bainite to occur. Increasing the sintering temperature means that the furnace cooling time under nitrogen is extended allowing more time for nucleation of bainite. After cooling from a sintering temperature of 1300°C, the transformation to bainite is almost complete.

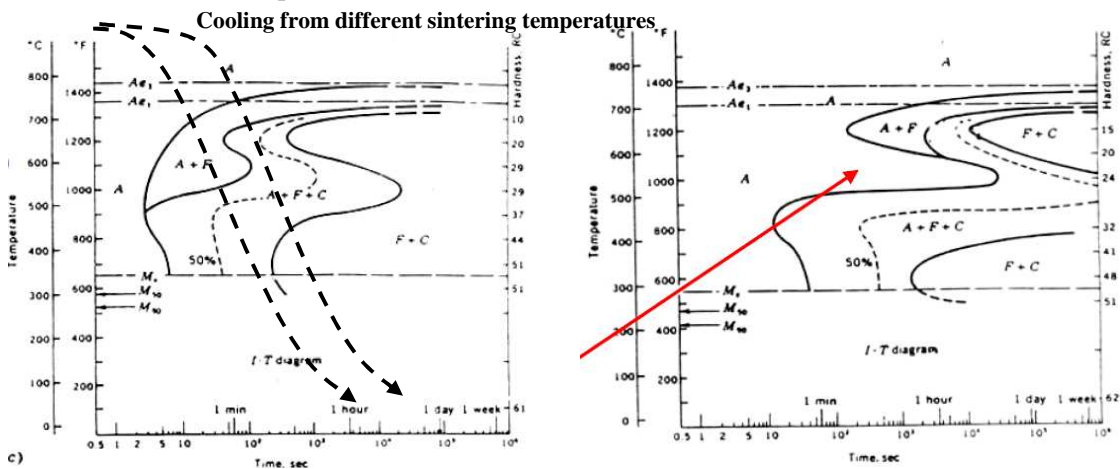


Figure 5: Time-Temperature-Transformation diagrams for (a) 4140 and (b) 4340. Arrow in figure (b) indicates the separation of the pearlite and bainite nose

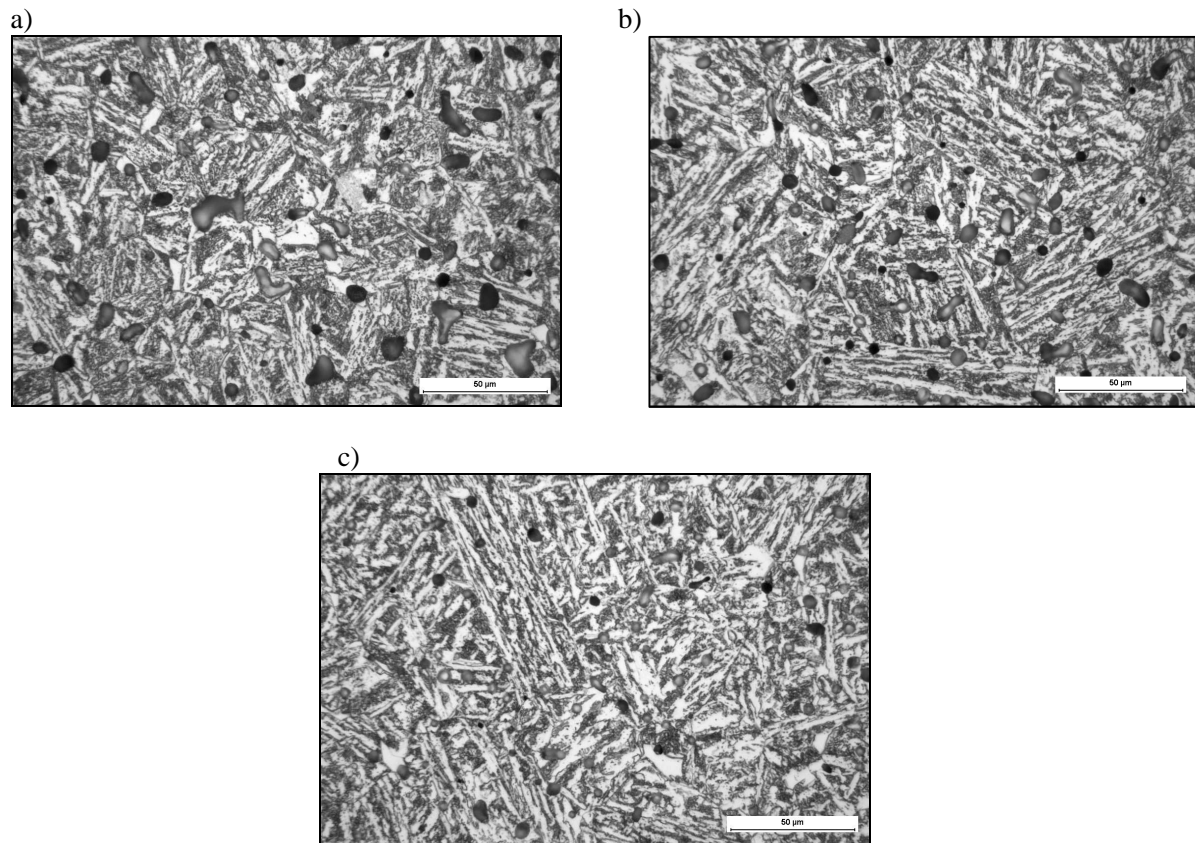


Figure 6: shows the effects of changing particle size distribution and MA+CIP vs. PA 4140 powders on as-sintered microstructures following sintering at 1300°C where the powder used is a) 90%-16µm (b) 90%-22µm (c) MA+CIP.

Figure 6 shows the effect of sintering at 1300°C on microstructure of PA powder with different particle sizes and MA+CIP where the powder used is a) 90%-16µm b) 90%-22µm c) MA+CIP. From this it is evident that both PA powders exhibited fully bainitic microstructures at this sinter temperature whereas the MA+CIP still has islands of surface pearlite. This suggests that there is not sufficient time for full diffusion of the master alloy during sintering.

Etched microstructures for 4340 MA+CIP are shown in Figure 7 as a function of sintering temperature. Following sintering at 1000°C there are still large particles of MA present, in a largely bainite matrix, that have not fully diffused. Unlike the 4140 the microstructure alloy 4340 is almost fully bainitic at 1100°C. This may be understood from the TTT diagram Figure 5 (b) where the arrow indicates a separation of the bainite and pearlite nose on the transformation curve. Pearlite is much harder to form in this alloy and this is reflected its absence from the microstructures shown in Figure 7.

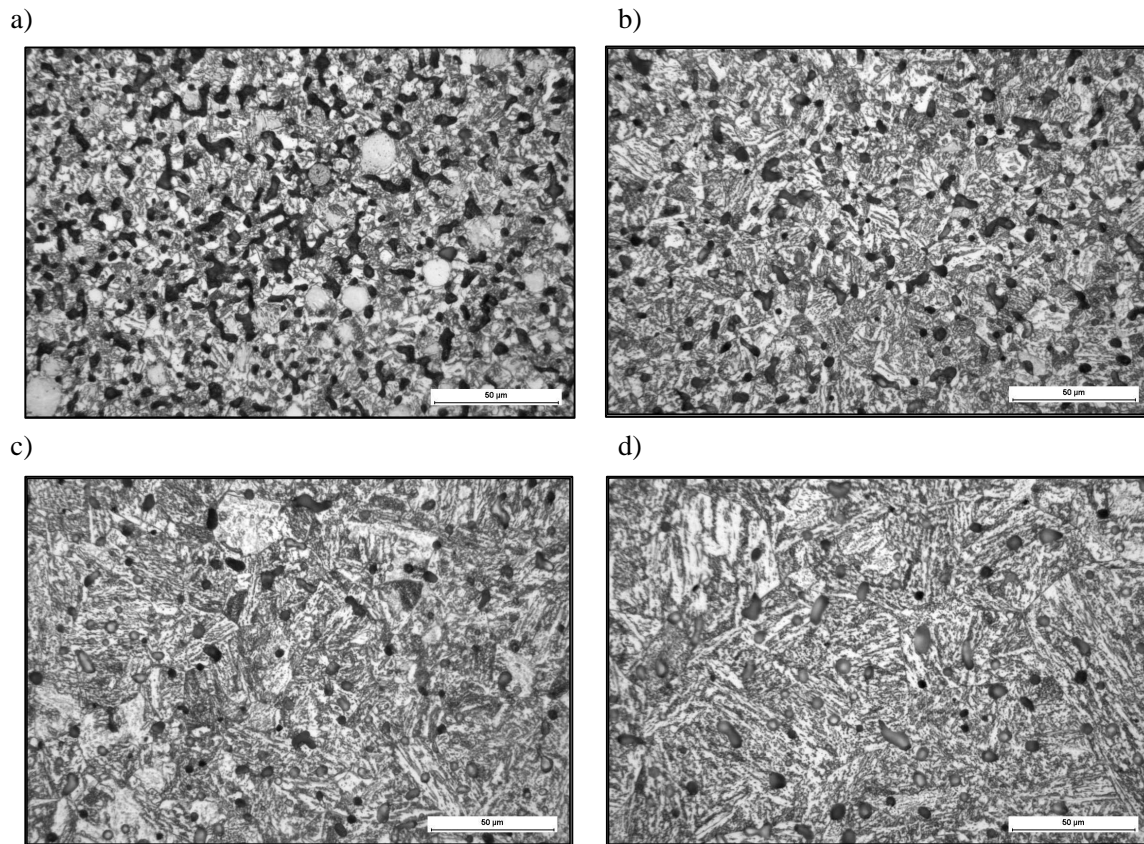


Figure 7: shows the effects of changing sintering temperature on as-sintered microstructure of MA+CIP 4340 a), 1000°C b), 1100°C c), 1200°C and d), 1300°C

Distortion

Distortion results for alloy 4340 Charpy bars sintered at 1100°C are shown in Figure 8. There is a noticeable reduction in distortion as the particle size distribution of the PA powder is reduced from 90%-22µm to 90%-16µm. However, the Charpy bar made with MA+CIP shows minimal distortion compared with bars made with the PA powders. The same observation was made for alloy 4140. While there is undoubtedly a beneficial effect associated with the high surface area of the CIP powder, the observed trend is probably accentuated by the fact that a fixed powder loading of 61.8wt% was adopted for all variants. The higher tap density of the 90%-22µm PA product means that the inter-particle binder width will on average be higher than for the MA+CIP variant and this will tend to increase mobility in the green part.



Figure 8: Distortion of 4340 following sintering at 1100°C. Powder particle size distributions are indicated alongside images.

Mechanical Properties

Hardness values for heat treated alloys 4140 and 4340 are shown in Figure 9. For both alloys the MA+CIP powders recorded the highest hardness values with peak or close to peak hardness achieved at 1200°C. Peak as-sintered hardness of 253Hv (23HRC) was recorded for alloy 4140 following sintering at 1300°C. The 90%-16µm PA powder achieved peak or close to peak hardness at 1100°C but peak hardness values were lower than those of MA+CIP. Hardness values for 4340 made via MA+CIP were slightly higher than 4140 values made via MA+CIP at all sintering temperatures.

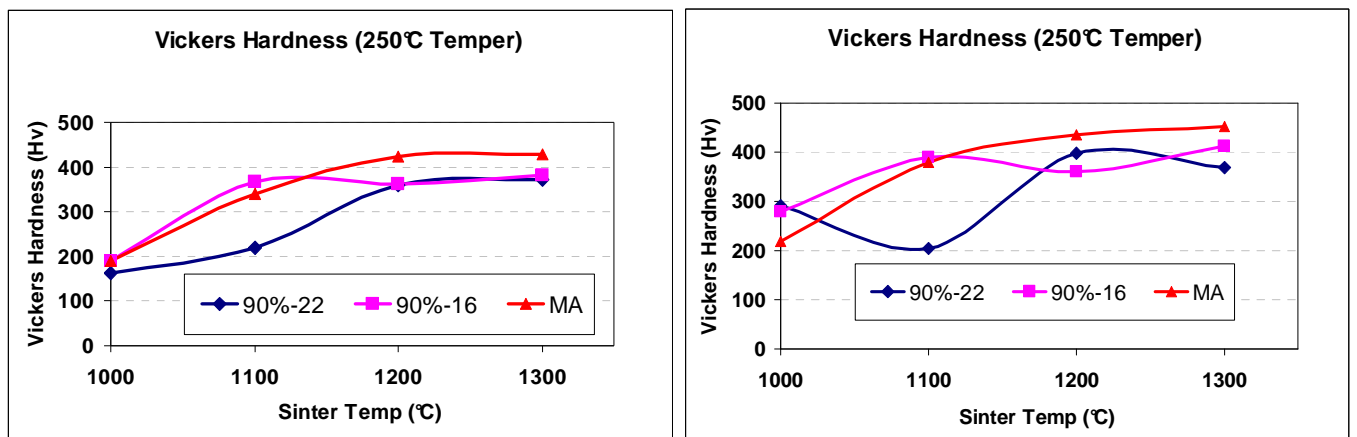


Figure 9: Vickers hardness (Hv) values for alloy a) 4140 and b) 4340 following tempering at 250°C and 230°C respectively for 1 hour

Tensile strength data for as-sintered alloy 4140 samples is shown in Figure 10. For all variants, tensile strength increased with increasing sintering temperature, with the smallest increase occurring between 1200°C and 1300°C indicating peak strength is being reached. The MA+CIP powder recorded the highest values for all sintering temperatures >1000°C. Following heat treatment, the MA+CIP powder showed a pronounced difference in behaviour over the PA powders. Values of UTS and 0.2% proof stress (not shown here) achieved peak tempered strength levels at significantly lower sintering temperature. For example, strength levels measured on samples sintered at 1100°C were greater than, or equal to the maximum PA values observed on samples sintered at 1300°C. The peak tempered strength is approximately double the as-sintered strength levels.

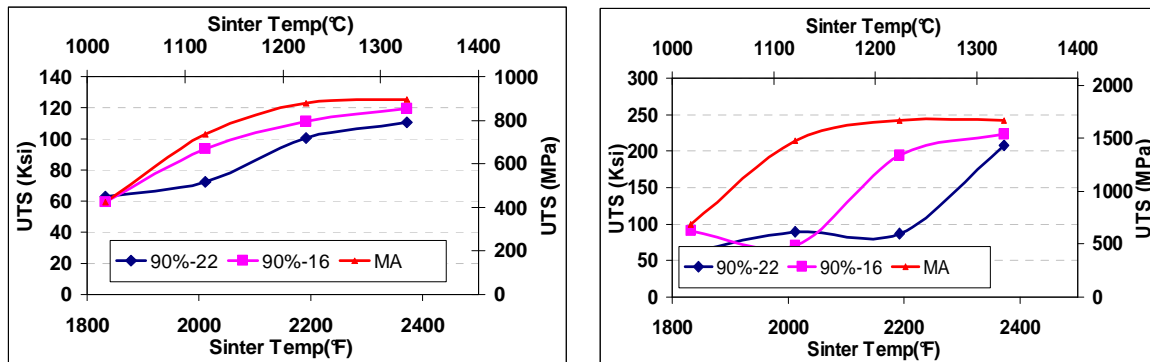


Figure 10: UTS values for alloy 4140 in the a), as-sintered and b), tempered at 250°C for 1 hour condition

At the time of publication the full data set of mechanical properties for 4340 samples is not available but preliminary 0.2%PS results for heat treated samples sintered 1300°C are 1145MPa, 1180MPa and 1218MPa for 90%-22 μ m, 90%-16 μ m and MA+CIP powder respectively.

DISCUSSION

The alloys chosen for this study are two of the more popular low alloy steels currently used within the MIM sector. Commercially, the 90%-22 μ m powder is most popular but the 90%-16 μ m powder provides a good comparison with the particle size distribution obtained from the MA+CIP powder. The powder size data shown in Table 4 shows expected trends in size distribution and while the D_{90} values are quite similar for the 90%-16 μ m PA and MA+CIP, the really significant difference behind sintering activity is seen in the D_{10} values which are 4.5 and 2.9 μ m respectively.

The fixed powder loading (61.8wt%) used in this study means that the inter-particle spacing will be smaller for the finer powders which have lower tap density. This is reflected in melt viscosity measurements (Table 4) and in the lower distortion for both alloys shown in Fig. 7 for 4340. Lower distortion is one of the major advantages of using MA+CIP over PA powder and was evident across the range of sintering temperatures investigated.

MIM values obtained in this study for MIM alloys 4140 and 4340 are in general better than or similar to mechanical property values reported elsewhere [4 – 8] (see Table 1,2) – particularly for 4140. Comparison with wrought properties highlights significant differences particularly in ductility (typically a few% elongation to failure in this study) and hence UTS which can reach much higher values because of lower (zero) porosity levels. Note that hot isostatic pressing can be applied to MIM parts as a post treatment to remove porosity and achieve superior properties. However, it is used only in a minority of cases and for most applications, the MIM'ed values are sufficient for purpose.

To summarise the findings of this study with respect to processing conditions that lead to properties exceeding published values for alloy 4140, Figure 11 has been constructed showing the matrix of variables giving properties exceeding these values. Matrices are shown for (a), as-sintered and (b), tempered conditions.

It should be noted that while mechanical property levels are met at low sintering temperature, the microstructure of the MA+CIP products achieves a homogeneous appearance only at > 1100°C. It is therefore important that this threshold is exceeded before parts enter service otherwise there is the risk that hard spots and localized corrosion will have deleterious consequences on performance. It should also be noted that the presence of pearlite in MA+CIP 4140 microstructure will reduce ductility.

The findings of this study concur with those of previous authors [2, 3] showing that the use of MA+CIP powder enables improved control of product chemistry (C,Cr,Mo,Mn and Si). This offers users the ability to achieve better control of the sintering process providing a more consistent product.

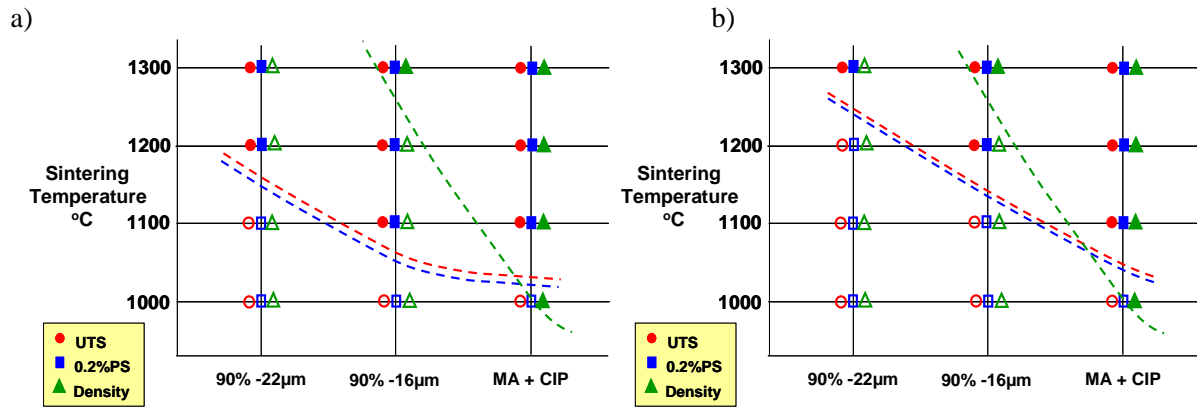


Figure 11: Matrix of conditions giving properties greater than a), as-sintered and b), heat treated published values. Values > published values are indicated by solid symbols.

In the case of 4340 the full data set is not available. However, porosity measurements are higher than would be expected following sintering, even at the highest sintering temperature. The high level of porosity translates into lower than expected mechanical properties when compared with published values shown in Table 2. This is perhaps a reflection of the potential difficulties in sintering these alloys and further work is required by the authors to optimise the sintering profile to reduce porosity.

SUMMARY & CONCLUSIONS

This study has demonstrated that PA and MA+CIP feedstocks can be processed successfully to deliver mechanical properties exceeding published values for MIM products. The process window for the 4140 MA+CIP product is however significantly wider than for the PA with sintering temperatures as low as 1100°C able to give acceptable properties whereas >1200°C is required to assure that the PA reaches published levels. This is attributed to the earlier onset of sintering promoted by fine CIP powder leading to earlier densification. For the MA+CIP variants, it is important that the sintering cycle is also designed to achieve a homogeneous microstructure before service.

The MA+CIP route offers advantages in terms of lower distortion compared with the PA powder products for a fixed powder loading. This trend requires further examination at a range of powder loading levels.

Higher than expected porosity levels in 4340 alloy are thought to have had a deleterious effect on mechanical properties reported. Further work is ongoing to improve the as-sintered properties of this alloy. Tempering at 250°C leads to a doubling of the strength levels of 4140 and ~60% increase for alloy 4340.

Ultimately the choice of PA vs MA will depend on the preferences of different MIM houses. Some are familiar with PAs, understand their behaviour well and may prefer not to have to carry out an additional blending operation with CIP. For those who may be considering MA but are concerned about control of carbon if using the MA+CIP route, this study shows that this is readily controllable. Moreover, for low alloy steels there could be cost advantages in using MA, as well as advantages in lower distortion and superior mechanical properties to be derived from the MA route.

ACKNOWLEDGEMENTS

Thanks are due to Dr Joe Strauss of HJE Co, Inc., for supporting dilatometry studies and to Ms. Linn Larsson of Sandvik Materials Technology, Sandviken, for coordinating metallographic studies.

REFERENCES

1. R. E. Wiech: U. S. Patent 4,602,953 (1986)
2. T.A. Tingskog, G.J. Del Corso, M.L. Schmidt and D.T. Whychell, “ Diffusion of Alloying Elements During Sintering of MIM Master Alloys”, Advances in Powder Metallurgy & Particulate Materials – 2002. Proceedings of the 2002 International Conference on Powder Metallurgy & Particulate Materials, Part 10, 156
3. P.A. Davies, G.R. Dunstan, D.F. Heaney and T.J. Mueller, “Comparison of Master Alloy and Pre-Alloyed 316L Stainless Steel Powders For Metal Injection Molding (MIM)”, PM2TEC 2004 World Congress, MPIF, Chicago, IL.
4. Metal Injection Moulding: A Manufacturing Process for Precision Engineering Components, EPMA
5. Catamold ® 42CrMo4 Data Sheet, 2006, BASF
6. Injection Molding of Metals & Ceramics, R M German & A Bose MPIF, 1997
7. http://www.efunda.com/materials/alloys/alloy_steels/alloy.cfm, accessed 14th April 2011
8. Catamold ® 4340 Data Sheet, 2006, BASF